



Aero-structural optimization of wind turbine blades using a reduced set of design load cases including turbulence

Sessarego, Matias; Shen, Wen Zhong

Published in:
Journal of Physics: Conference Series

Link to article, DOI:
[10.1088/1742-6596/1037/4/042018](https://doi.org/10.1088/1742-6596/1037/4/042018)

Publication date:
2018

Document Version
Publisher's PDF, also known as Version of record

[Link back to DTU Orbit](#)

Citation (APA):
Sessarego, M., & Shen, W. Z. (2018). Aero-structural optimization of wind turbine blades using a reduced set of design load cases including turbulence. *Journal of Physics: Conference Series*, 1037(4), Article 042018. <https://doi.org/10.1088/1742-6596/1037/4/042018>

General rights

Copyright and moral rights for the publications made accessible in the public portal are retained by the authors and/or other copyright owners and it is a condition of accessing publications that users recognise and abide by the legal requirements associated with these rights.

- Users may download and print one copy of any publication from the public portal for the purpose of private study or research.
- You may not further distribute the material or use it for any profit-making activity or commercial gain
- You may freely distribute the URL identifying the publication in the public portal

If you believe that this document breaches copyright please contact us providing details, and we will remove access to the work immediately and investigate your claim.

PAPER • OPEN ACCESS

Aero-structural optimization of wind turbine blades using a reduced set of design load cases including turbulence

To cite this article: Matias Sessarego and Wen Zhong Shen 2018 *J. Phys.: Conf. Ser.* **1037** 042018

View the [article online](#) for updates and enhancements.

Related content

- [Study on Determination Method of Fatigue Testing Load for Wind Turbine Blade](#)
Gaohua Liao and Jianzhong Wu
- [Finite Element Analysis for the Web Offset of Wind Turbine Blade](#)
Bo Zhou, Xin Wang, Changwei Zheng et al.
- [Wireless Sensors for Wind Turbine Blades Monitoring](#)
N Iftimie, R Steigmann, N A Danila et al.

Aero-structural optimization of wind turbine blades using a reduced set of design load cases including turbulence

Matias Sessarego and Wen Zhong Shen

Department of Wind Energy, Technical University of Denmark, Lyngby Campus, 2800 Kgs. Lyngby, Denmark.

E-mail: matse@dtu.dk

Abstract. Modern wind turbine aero-structural blade design codes generally use a smaller fraction of the full design load base (DLB) or neglect turbulent inflow as defined by the International Electrotechnical Commission standards. The current article describes an automated blade design optimization method based on surrogate modeling that includes a very large number of design load cases (DLCs) including turbulence. In the present work, 325 DLCs representative of the full DLB are selected based on the message-passing-interface (MPI) limitations in Matlab. Other methods are currently being investigated, e.g. a Python MPI implementation, to overcome the limitations in Matlab MPI and ultimately achieve a full DLB optimization framework. The reduced DLB and the annual energy production are computed using the state-of-the-art aero-servo-elastic tool HAWC2. Furthermore, some of the interior dimensions of the blade structure are optimized using the finite-element based cross-sectional analysis tool BECAS. The optimization framework is applied to redesign the NREL 5 MW wind turbine blade to obtain improvements in rotor performance and blade weight.

1. Introduction

Modern wind turbine aero-structural blade design codes generally use a smaller fraction of the full design load base (DLB) defined by the International Electrotechnical Commission (IEC) standards. The difficulty with implementing a full DLB in an optimization framework includes 1) the high computational cost of running a full DLB for each change of a design variable, and 2) the non-deterministic nature of design load cases (DLCs) that include turbulence, which introduces non-smoothness in the objective function and may cause gradient-based optimization methods to stop prematurely.

One of the most comprehensive and detailed rotor design frameworks is **Cp-Max** developed by Bottasso [1]. To compute the annual energy production (AEP) and the DLCs, **Cp-Max** uses **Cp-Lambda**, which consists of blade element momentum (BEM) and geometrically exact beam theory for the aerodynamic and structural-dynamic modeling, respectively. The finite-element-method (FEM) cross-sectional model ANBA is used for the structural analysis. In addition to ANBA, a fully resolved 3D FEM package, MSC Nastran, is used to make the structural design as realistic as possible.

Zahle et al. [2] described an integrated multi-disciplinary wind turbine optimization framework using state-of-the-art aero-elastic and structural tools: HAWC2 [3], HAWCStab2 [4],



and BECAS [5]. The optimization framework, called `HAWT0pt2`, uses OpenMDAO to handle the definition of the optimization problem, work flow, data flow, and parallelization of simulation cases. The optimization algorithm used is the open source gradient-based interior point optimizer IPOPT. Pavese et al. [6] developed a reduced DLB for multidisciplinary design optimization (MDO) frameworks. The aim of the reduced DLB is to provide a fast and reliable alternative to computing the full DLB for the estimation of ultimate blade loads in an MDO framework. The reduced DLB was implemented in `HAWT0pt2` to redesign the DTU 10 MW wind turbine rotor.

In previous works, e.g. [1] and [2], DLCs are carefully selected to incorporate different important operating and environmental states that the wind turbine will encounter in practice. The DLCs are down-selected for a design context based on their import for the design objective and not based on computational limitations nor code stability. The current article focuses on quantity rather than quality. The contribution of the current article is to describe a method to design wind turbine blades that allows the computation of a very large number of DLCs directly including turbulent inflow. The method presented, which builds a surrogate model, can be considered an advancement compared to the other existing methods because the method can handle more DLCs including turbulent inflow.

The full DLB is not computed here for two reasons: 1) the presented Matlab MPI implementation is limited to a certain number of processors, and 2) some DLC simulation runs crash for certain blade shapes and are difficult to deal with in the optimizer. The second point could be addressed by emphasizing feasible blade shapes, e.g. by using stricter constraints on chord, twist, and thickness. Nevertheless, in the present work a representative set consisting of 325 DLCs is used instead. Depending on the wind turbine though, the number of DLCs may be slightly larger or smaller than 325. Other methods are currently being investigated, e.g. a Python MPI implementation, which may allow more than 325 DLCs to be computed.

The following text describes the blade design framework and the application of the framework for the blade redesign of the NREL 5 MW wind turbine. Finally, conclusions are given.

2. Methodology

The methodology section contains three subsections: 1) Problem definition, 2) optimization layout, and 3) optimization algorithm. Figure 1 is a flowchart and may assist in understanding the subsections.

2.1. Problem definition

The blade design framework consists of the following wind turbine modeling tools: HAWC2, HAWCStab2 [4], and BECAS developed at Risø Campus, Technical University of Denmark. To estimate the cost of energy (COE), the wind turbine design cost and scaling model developed at NREL [7] is employed. Message-passing-interface (MPI) parallelization is performed using pMatlab developed at the Lincoln Laboratory, Massachusetts Institute of Technology [8], and finally a surrogate-based optimization code as described in [9] is used to solve Problem (1).

The design objective is to minimize the COE:

$$\begin{aligned}
 & \underset{\mathbf{x}}{\text{minimize}} && \text{COE} \\
 & \text{subject to} && \mathbf{x} \in \mathbb{R}^n, \\
 & && g_c(\mathbf{x}) \leq 0, \\
 & && x_k^L \leq x_k \leq x_k^U, k = 1, \dots, n
 \end{aligned} \tag{1}$$

where the vector \mathbf{x} contains a total of n variables that are real numbers, \mathbb{R} . The design variables, $\mathbf{x} = [x_1, x_2, \dots, x_n]$, are control points (CPs) that define the chord, twist and relative thickness as a function of blade span, see Figure 2. B-splines are used to parameterize the chord and twist

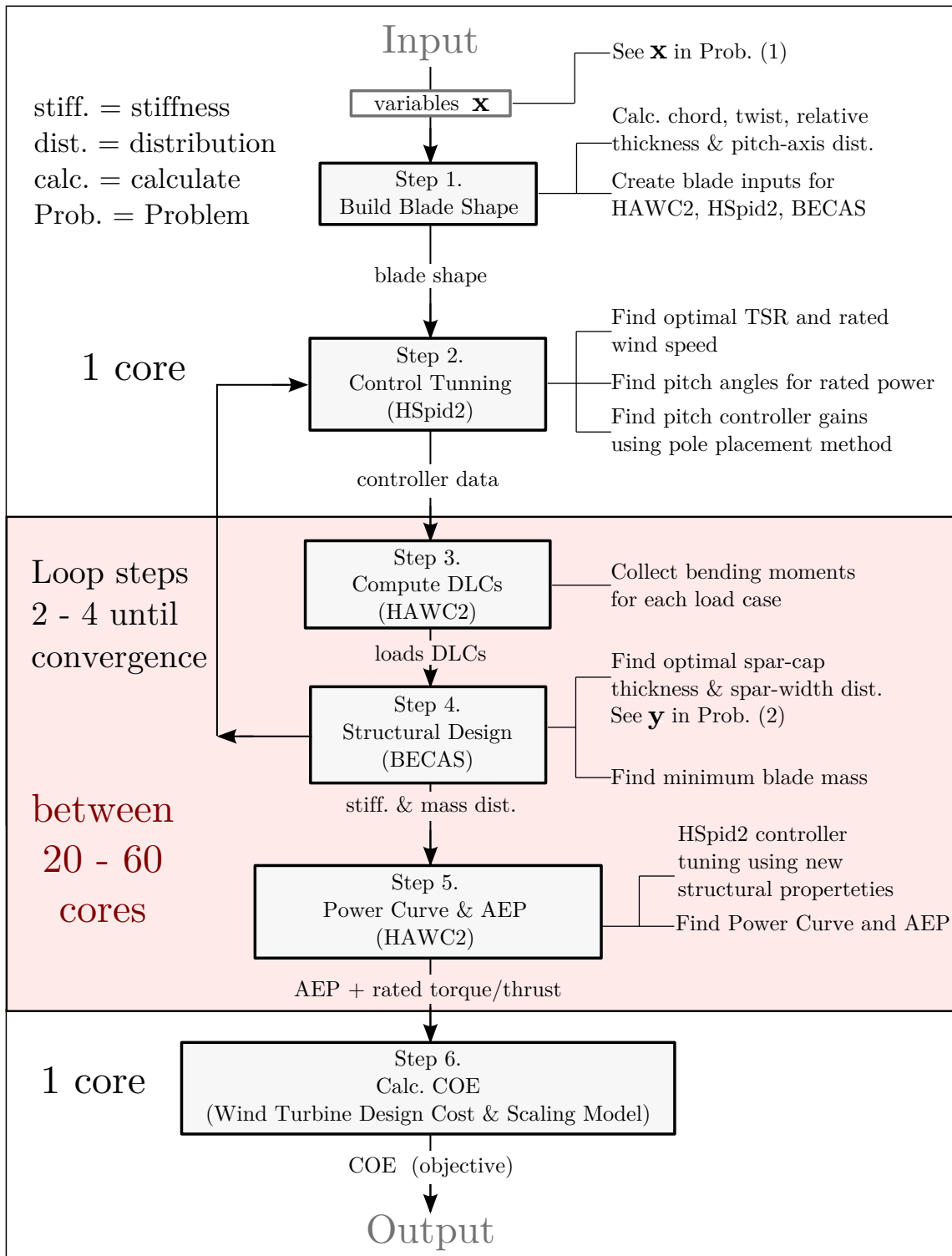


Figure 1: Flowchart for evaluating a candidate blade design comprised of six steps: 1) Build blade shape, 2) control tuning, 3) compute DLCs, 4) structural design, 5) re-tune and compute AEP, and 6) calculate COE.

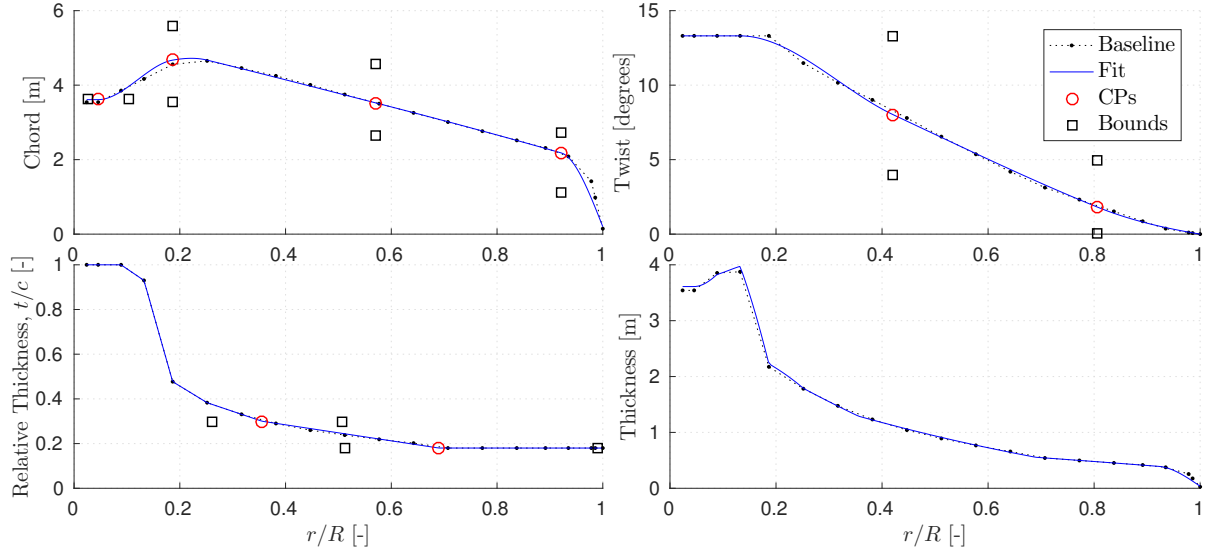


Figure 2: NREL 5 MW wind turbine blade with baseline (dashed) and fitted (line) geometries. The circles and squares represent the CPs and upper/lower bounds, respectively.

distributions, while linear interpolation is used for the relative thickness distribution. Only four CPs for the chord, two CPs for twist, and two CPs for the relative thickness distributions are optimized. The total number of variables is then eight. The upper (U) and lower (L) notations, $x_k^L \leq x_k \leq x_k^U$, are the upper and lower bounds of the CPs, while the non-linear inequality constraint, $g_c \leq 0$, is used to promote feasible blade designs (e.g. a constraint on maximum rated thrust).

An optimization tool to design the internal structure of the blade is included in the framework. The tool uses a combination of BECAS to compute the blade structural properties, stress and strain, the Euler-Bernoulli beam theory to compute blade natural frequencies and deflections, and HAWC2 to compute the 325 DLCs. The *fmincon* [10] optimizer in Matlab is used to minimize the blade mass subject to a number of boundary and non-linear inequality constraints to promote blade structural feasibility:

$$\begin{aligned}
 & \underset{\mathbf{y}}{\text{minimize}} && \text{Blade Mass} \\
 & \text{subject to} && \mathbf{y} \in \mathbb{R}^n, \\
 & && (3\omega_{\text{rotor}} SF - \omega(\mathbf{y}))/\omega_{\text{rotor}} \leq 0, \\
 & && (\delta_{\text{tip}}(\mathbf{y}) - \delta_{\text{max}})/\delta_{\text{max}} \leq 0, \\
 & && (\epsilon_{\text{tension}}(\mathbf{y}) SF - \epsilon_{\text{ultimate,tension}})/\epsilon_{\text{ultimate,tension}} \leq 0, \\
 & && (\epsilon_{\text{compression}}(\mathbf{y}) SF - \epsilon_{\text{ultimate,compression}})/\epsilon_{\text{ultimate,compression}} \leq 0, \\
 & && (\eta(\mathbf{y}) - \eta_{\text{max}})/\eta_{\text{max}} \leq 0, \\
 & && y_k^L \leq y_k \leq y_k^U, k = 1, \dots, n
 \end{aligned} \tag{2}$$

where $3\omega_{\text{rotor}}$ is the rotor blade passing frequency, SF is a safety factor, δ_{max} is the maximum allowable tip deflection, $\epsilon_{\text{ultimate,tension}}$ and $\epsilon_{\text{ultimate,compression}}$ are the ultimate tensile and compressive strain, respectively, and η_{max} is the maximum allowable buckling coefficient set to 0.5. The buckling coefficient, η , is computed for the spar-caps only, and assumes that the spar-beam is modeled as a long orthotropic plate under uni-axial compression with all edges simply supported [11]. Skin and panel buckling are not considered. The tip deflection, δ_{tip} ,

as well as the natural frequencies for the first flap-wise and edge-wise blade modes, ω , are calculated from Euler-Bernoulli beam theory. The tensile ($\epsilon_{\text{tension}}$) and compressive ($\epsilon_{\text{compression}}$) strain are computed at the element centers in the cross-section finite-element mesh. Fatigue and more accurate methods for calculating tip deflection, natural frequencies, and the buckling are neglected to reduce the computational cost. All constraints are scaled to prevent bias and improve optimizer performance.

A box-spar layout is assumed for the internal blade structure, where the design variables are the spar-cap thickness and web layout (or spar width) across the blade span, see Figures 3 and 4. The spar-cap thickness distribution is defined by six CPs, while the web layout is defined by four CPs for a two-web layout. Upper and lower bounds of the spar-caps and webs are used to prevent them from merging into each other and into different sectors of the cross-section, as well as becoming negative. The thickness of the upper and lower spar-caps are identical.

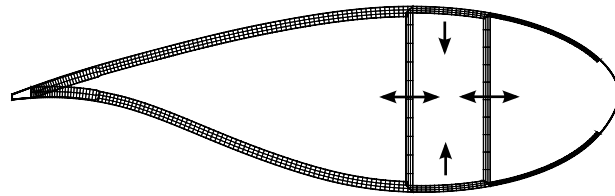


Figure 3: Two-dimensional finite-element mesh of a NREL 5 MW blade cross-section. The spar-cap thickness changes following the up/down arrows, while the webs can move left or right.

2.2. Optimization layout

The structural design code begins by tuning the generator and pitch controller using HSpid2. HSpid2 is the free and reduced version of HAWCStab2, whose sole purpose is to provide tuning parameters for a PI controller [4]. Then, a series of DLCs based on Class IB (or any other class) of the IEC 61400-1 standards [12] are computed, see Table 1. Fatigue and load extrapolations are neglected and only ultimate loads (Ult.) with a safety factor of 1.755 for all DLCs are considered. The flapwise and edgewise bending moments in all sections on all three blades for all the DLCs are collected and placed inside a convex hull. The worst-case loads, represented

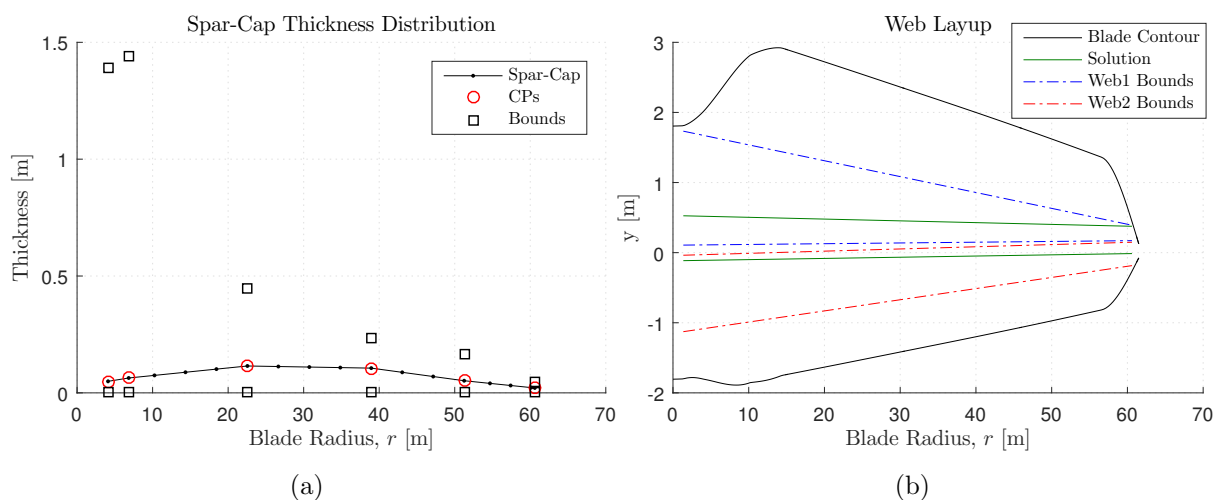


Figure 4: (a) Spar-cap thickness and (b) web layout for the baseline fit blade geometry.

by the edges of the convex hull, are sent to the optimizer, which calls a structural module for a number of iterations to find the minimum blade mass. The inputs to the structural module are the DLC loads and \mathbf{y} . The vector \mathbf{y} is used to create a structural layout and compute the objective, while the DLC loads together with the blade structural properties are used to compute the structural constraints. The Matlab optimizer, *fmincon*, modifies \mathbf{y} to minimize the objective up to at least a local minimum and also satisfy all constraints.

The design of the controller and the DLC computations are based on the baseline turbine, but with a modified outer geometry, see Figure 1. In other words, the stiffness distributions of the baseline blade are kept to tune the controller and compute the DLCs. In a fully aero-elastic design approach, Steps 2 to 4 should be repeated until convergence, where the blade stiffness distributions found from Step 4 are used to update the stiffness distributions used in Steps 2 and 3. Performing the fully aero-elastic design approach increases the complexity, the computational cost and the probability that the framework will crash. Therefore, the fully aero-elastic design was omitted in the present work for simplicity, faster code execution, and robustness.

2.3. Optimization algorithm

A surrogate-based optimization approach developed by the authors [9] is employed, which uses a mathematical model for searching local or global optima rather than the black-box function directly [13]. In general, surrogate-based optimization consists of three steps to find the minimum of a function:

- (i) creating a sampling plan;
- (ii) constructing a surrogate, and;
- (iii) searching and exploiting the surrogate.

The sampling plan is created using the Latin hypercube sampling technique [9, 14], the surrogate is constructed using a radial basis function, and prediction-based exploitation [9, 14] is used to search and exploit the surrogate. A radial basis function is expressed as:

$$\hat{f}(\mathbf{x}) = \mathbf{w}^T \boldsymbol{\psi} = \sum_{i=1}^{n_c} w_i \psi(\|\mathbf{x} - \mathbf{c}^{(i)}\|) \quad (3)$$

where \hat{f} is the surrogate approximation to the scalar-valued objective function, f (see Problem (1)), \mathbf{x} is the design variable vector, \mathbf{w} is a vector containing the values of the weight coefficients w_i from $i = 1, \dots, n_c$, and $\boldsymbol{\psi}$ is the n_c -vector containing the values of the basis functions ψ . A cubic basis function, $\psi(r_b) = r_b^3$, is used where $r_b = \|\mathbf{x} - \mathbf{c}^{(i)}\|$ is from Equation 3. The values of the basis functions are evaluated at the Euclidean distances between the prediction site \mathbf{x} and the centers $\mathbf{c}^{(i)}$ of the basis functions. A unique solution for \mathbf{w} in the above equation can be determined when n_c is equal to the number of sampled points and using the *Gram matrix* [14]. Each candidate blade design in steps i) and iii) above goes through six stages to determine the COE, see Figure 1. In the present work, the sampling plan consists of 28 distinct blade shapes, see Figure 5, and 10 iterations are used in the prediction-based exploitation scheme. The total number of function evaluations is then 38. For the optimization performed in section 3, the number of surrogate evaluations in the prediction-based exploitation is 21,413.

3. Results

Airfoils are comprised of a cylinder, Delft University (DU) airfoils, and a NACA airfoil as described in [15]. The reference structural layout, safety factors, strain and tip deflection limits are obtained from [16]. Rotor radius and tip speed are kept the same throughout the optimization. A Weibull probability distribution with shape and scale parameters of $k = 2.47$

Table 1: Design load cases (DLCs) from the International Electrotechnical Commission standards [12]. The *Treated* column describes how the DLC is treated. Fatigue and load extrapolations are neglected and only ultimate loads (Ult.) with a safety factor of 1.755 for all DLCs are considered.

| Design situation | DLC | Wind condition | Other conditions | Type of analysis | Partial safety factor | Treated |
|--|-----|---|--|------------------|-----------------------|---------|
| 1) Power production | 1.1 | NTM $V_{in} < V_{hub} < V_{out}$ | For extrapolation of extreme events | U | N | Yes |
| | 1.2 | NTM $V_{in} < V_{hub} < V_{out}$ | | F | * | No |
| | 1.3 | ETM $V_{in} < V_{hub} < V_{out}$ | | U | N | Yes |
| | 1.4 | ECD $V_{hub} = V_r - 2 \text{ m/s}, V_r, V_r + 2 \text{ m/s}$ | | U | N | Yes |
| | 1.5 | EWS $V_{in} < V_{hub} < V_{out}$ | | U | N | Yes |
| 2) Power production plus occurrence of fault | 2.1 | NTM $V_{in} < V_{hub} < V_{out}$ | Control system fault or loss of electrical network Protection system or preceding internal electrical fault | U | N | Yes |
| | 2.2 | NTM $V_{in} < V_{hub} < V_{out}$ | | U | A | No |
| | 2.3 | EOG $V_{hub} = V_r \pm 2 \text{ m/s}$ and V_{out} | | U | A | Yes |
| | 2.4 | NTM $V_{in} < V_{hub} < V_{out}$ | | F | * | Ult. |
| 3) Start up | 3.1 | NWP $V_{in} < V_{hub} < V_{out}$ | | F | * | Ult. |
| | 3.2 | EOG $V_{hub} = V_{in}, V_r \pm 2 \text{ m/s}$ and V_{out} | | U | N | Yes |
| | 3.3 | EDC $V_{hub} = V_{in}, V_r \pm 2 \text{ m/s}$ and V_{out} | | U | N | Yes |
| 4) Normal shut down | 4.1 | NWP $V_{in} < V_{hub} < V_{out}$ | | F | * | Ult. |
| | 4.2 | EOG $V_{hub} = V_r \pm 2 \text{ m/s}$ and V_{out} | | U | N | Yes |
| 5) Emergency shut down | 5.1 | NTM $V_{hub} = V_r \pm 2 \text{ m/s}$ and V_{out} | | U | N | Yes |
| 6) Parked (standing still or idling) | 6.1 | EWM 50-year recurrence period | Loss of electrical network connection Extreme yaw misalignment | U | N | Yes |
| | 6.2 | EWM 50-year recurrence period | | U | A | Yes |
| | 6.3 | EWM 1-year recurrence period | | U | N | Yes |
| | 6.4 | NTM $V_{hub} < 0.7V_{ref}$ | | F | * | Ult. |
| 7) Parked and fault conditions. | 7.1 | EWM 1-year recurrence period | | U | A | Yes |
| 8) Transport, assembly, maintenance and repair | 8.1 | NTM V_{maint} to be stated by the manufacturer | | U | T | No |
| | 8.2 | EWM 1-year recurrence period | | U | A | No |

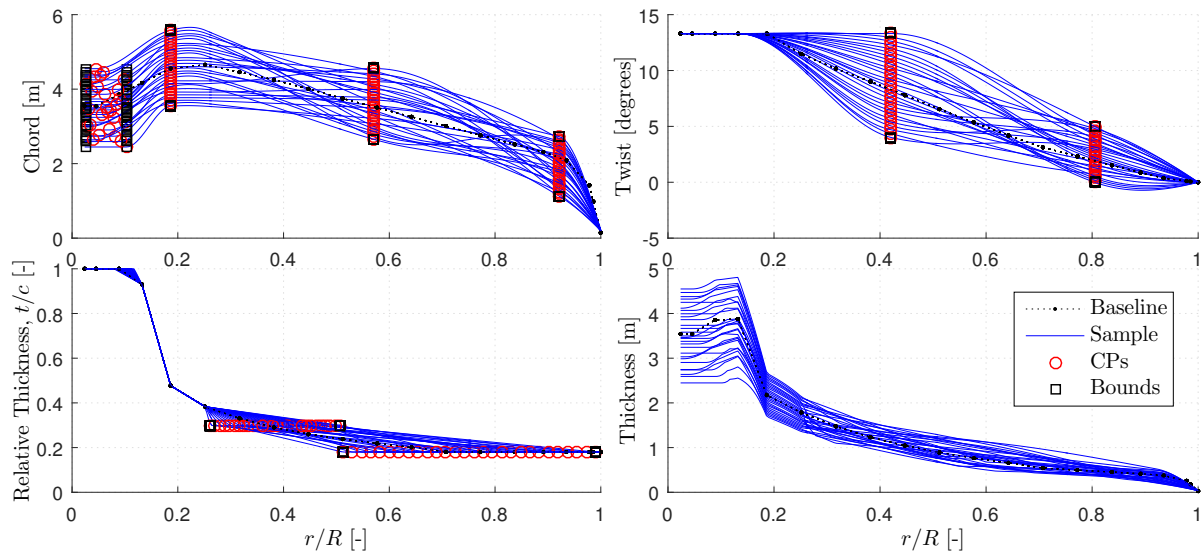


Figure 5: Twenty-eight distinct blade shapes created using the Latin hypercube sampling technique. The circles and squares represent the CPs and upper/lower bounds, respectively.

and $A = 9.49$ m/s, respectively, is used to calculate the AEP. Figure 2 depicts the NREL 5 MW wind turbine blade with the baseline (dashed) and fitted (line) geometries. Chord, twist, relative and dimensional thicknesses are plotted against the normalized radius r/R where $R = 63$ m. The circles and squares represent the CPs and upper/lower bounds, respectively.

Figure 6 depicts the baseline (dashed) and optimized (line) blade geometries. The three-dimensional views of the (a) baseline fit and (b) optimized blade geometries are displayed in Figure 7. In Figure 6, the optimized blade (Result) shows a smaller chord from root to tip compared to the baseline. Furthermore, there is less twist at approx. $r/R = 0.4$ and more twist at approx. $r/R = 0.8$. The relative thickness, defined as the dimensional thickness divided by the chord length, is larger than the baseline. A larger relative thickness indicates that thicker airfoils are used in the optimized blade geometry, possibly as a means to improve structural integrity and reduce blade mass. Although thicker airfoils are used, the dimensional thickness of the optimized blade is similar or less than the baseline due to the decrease in chord.

The (a) spar-cap thickness and (b) web layout for the baseline fit and optimized blade geometries are shown in Figures 4 and 8, respectively. Figure 4(a) and Figure 8(a) show that the spar-cap thickness for the optimized geometry is less than the baseline fit. Similarly, Figure 4(b) and Figure 8(b) show that the webs and spar-cap width are slightly narrower for the optimized geometry than the baseline fit. A comparison of the flapwise (FW) and edgewise (EW) bending, and torsional stiffness (stiff.) between the baseline fit and optimized blade geometries is shown in Figure 9. Mass per length is included in Figure 9 as well. Figure 9 shows a reduction in all quantities for the optimized geometry with respect to the baseline fit. Since the box-spar configuration is quite inflexible and the number of structural design variables is limited, the optimized blade is probably not structurally tailored to alleviate loads through torsional effects. A detailed analysis of the loads from the DLCs has not yet been conducted.

Table 2 contains the performance results for the baseline fit and optimized blade geometries. The optimized blade has 1.6% less COE (see Problem 1), 16.7% less thrust at rated wind speed, weighs 20.7% less, but produces 0.1% less AEP than the baseline fitted blade. In conclusion, except for the slight decrease in AEP, the optimization framework produced desired results.

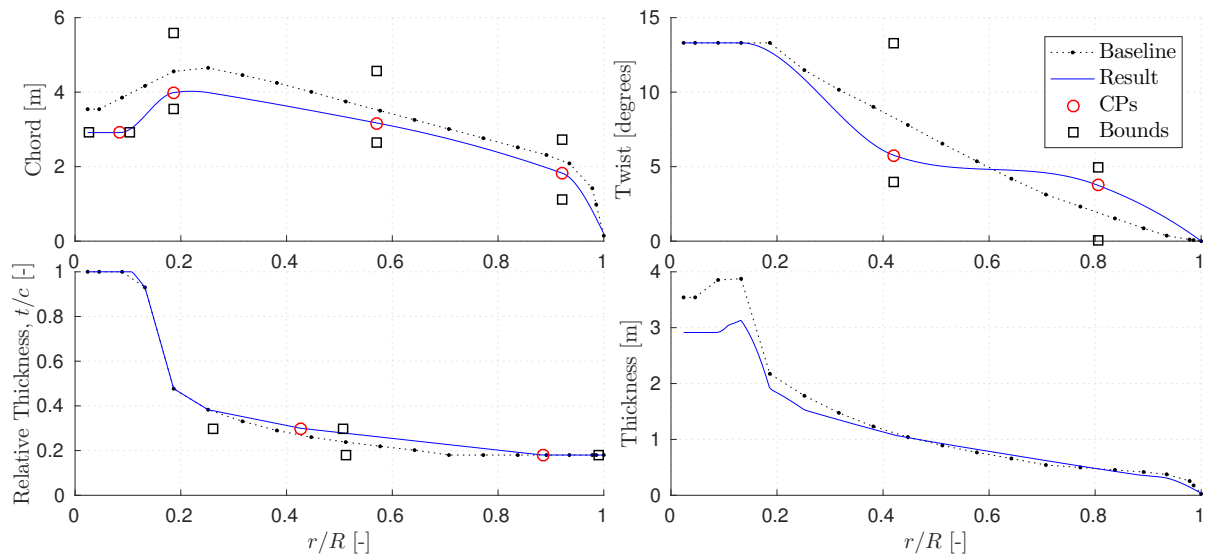


Figure 6: NREL 5 MW wind turbine blade with baseline (dashed) and optimized (line) geometries. The circles and squares represent the CPs and upper/lower bounds, respectively.

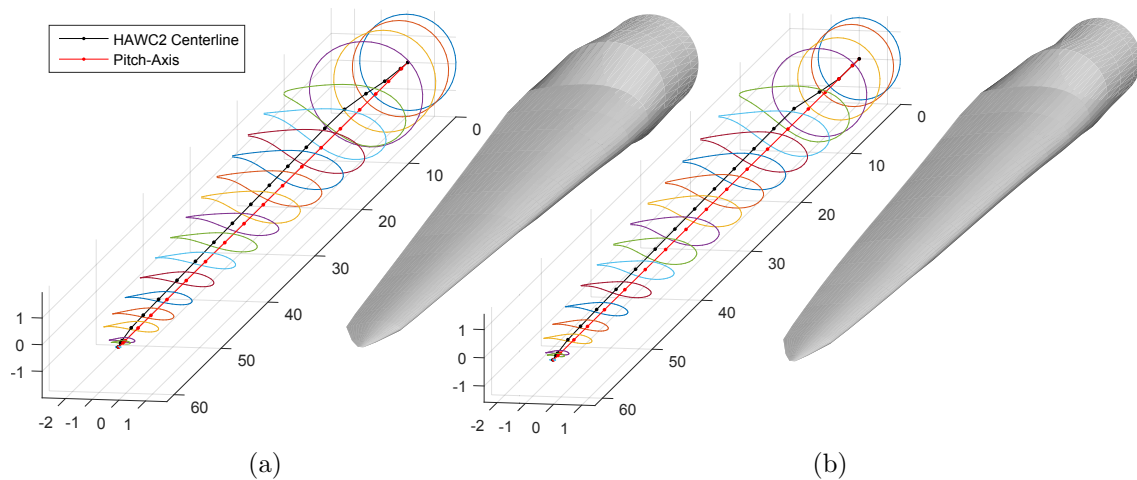


Figure 7: NREL 5 MW wind turbine blade with (a) baseline fit and (b) optimized geometries.

Table 2: Performance comparison between the baseline fit and optimized blades.

| Quantity | COE (USD/kWh) | AEP (GWh/Year) | Rated Thrust (kN) | Blade Mass (kg) |
|-----------------|------------------|-------------------|----------------------|--------------------|
| Baseline Fit | 0.0678 | 23.523 | 820.99 | 20,293 |
| Optimized | 0.0667 | 23.502 | 684.12 | 16,090 |
| Improvement (%) | +1.612 | -0.090 | +16.671 | +20.711 |

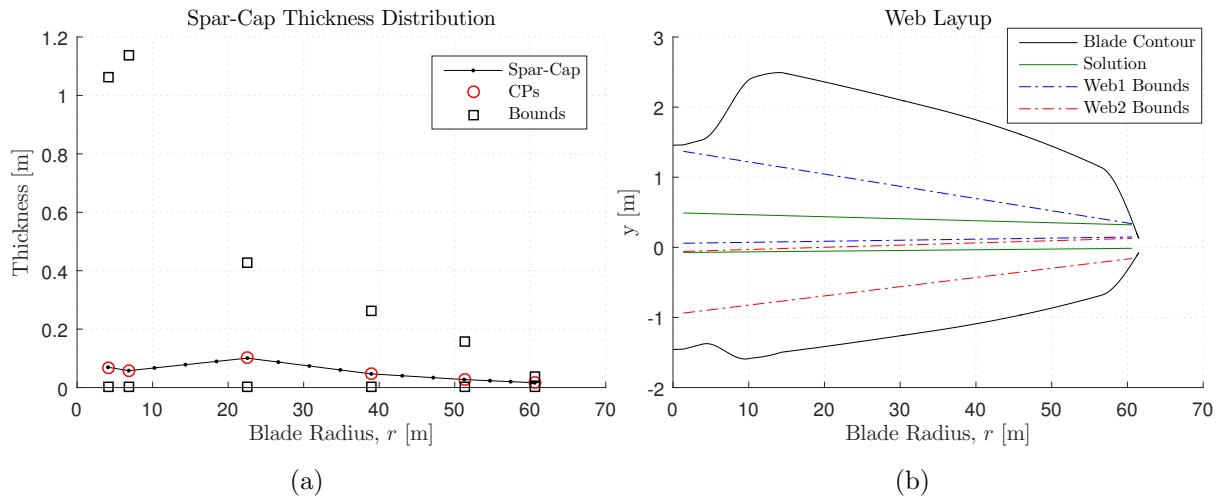


Figure 8: (a) Spar-cap thickness and (b) web layout for the optimized blade geometry.

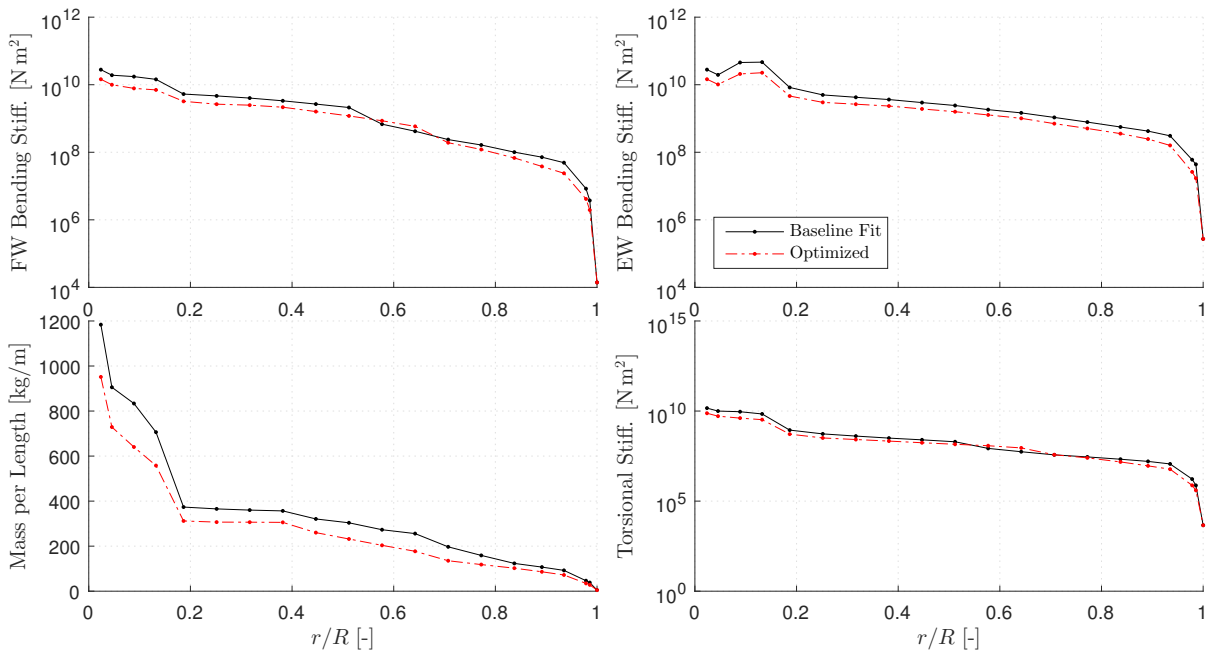


Figure 9: Comparison of the flapwise (FW) and edgewise (EW) bending, and torsional stiffness (stiff.) between the baseline fit and optimized blade geometries. Mass per length included as well.

4. Conclusions

Modern wind turbine aero-structural blade design codes generally use a smaller fraction of the full design load base (DLB) or neglect turbulent inflow as defined by the International Electrotechnical Commission standards. The current article describes an automated blade design optimization method that includes 325 design load cases (DLCs) including turbulence. The 325 DLCs are representative of the full DLB and were selected based on the message-passing-interface (MPI) limitations in Matlab. The reduced DLB and the annual energy production are computed using the aero-servo-elastic tool HAWC2. The interior dimensions of the blade

structure are optimized using the finite-element based cross-sectional analysis tool BECAS. The optimization framework is applied to redesign the NREL 5 MW wind turbine blade based on Class IB to obtain improvements in rotor performance and blade weight.

Acknowledgments

The present work was funded by the Danish Council for Strategic Research under the project name OffWindChina (Sagsnr. 0603-00506B). The support is gratefully acknowledged. Computations were performed on Jess, the high performance computing cluster at Risø Campus, Technical University of Denmark.

References

- [1] Bottasso C L, Bortolotti P, Croce A and Gualdoni F 2015 *Multibody System Dynamics* 1–28 ISSN 1573-272X URL <http://dx.doi.org/10.1007/s11044-015-9488-1>
- [2] Zahle F, Tibaldi C, Pavese C, McWilliam M K, Blasques J P A A and Hansen M H 2016 *Journal of Physics: Conference Series* **753** 062008 URL <http://stacks.iop.org/1742-6596/753/i=6/a=062008>
- [3] Larsen T J and Hansen A M 2007 *HAWC2 - User manual* DTU-Risø-R-1597
- [4] Lars Christian Henriksen C T and Bergami L 2015 *HAWCStab2 User Manual* DTU Wind Energy Technical University of Denmark, Frederiksborgvej 399 4000 Roskilde, Denmark
- [5] Blasques J P and Stolpe M 2012 *Composite Structures* **94** 3278 – 3289 ISSN 0263-8223 URL <http://www.sciencedirect.com/science/article/pii/S0263822312002085>
- [6] Pavese C, Tibaldi C, Larsen T J, Kim T and Thomsen K 2016 *Journal of Physics: Conference Series* **753** 062005 URL <http://stacks.iop.org/1742-6596/753/i=6/a=062005>
- [7] Fingerish L, Hand M and Laxson A 2006 Wind turbine design cost and scaling model Tech. rep. National Renewable Energy Laboratory 1617, Cole Blvd, Golden, CO 80401
- [8] Kim H, Mullen J and Kepner J *Introduction to Parallel Programming and pMatlab v2.0* MIT Lincoln Laboratory Lexington, MA 02420 accessed February 7, 2017. URL <http://www.ll.mit.edu/mission/cybersec/softwaretools/pmatlab/pmatlab.html>
- [9] Sessarego M, Ramos-García N, Yang H and Shen W Z 2016 *Renewable Energy* **93** 620 – 635 ISSN 0960-1481 URL <http://www.sciencedirect.com/science/article/pii/S0960148116302117>
- [10] The MathWorks Inc. Natick, MA *MATLAB 2014b*
- [11] Kassapoglou C 2010 *Buckling of Composite Plates* (John Wiley & Sons, Ltd) pp 119–144 ISBN 9780470972700 URL <http://dx.doi.org/10.1002/9780470972700.ch6>
- [12] 2005 *International Standard IEC 61400-1: Wind turbine - Part 1: Design requirements* 3rd ed IEC 61400-1:2005(E) (International Electrotechnical Commission) URL <https://webstore.iec.ch/publication/5426>
- [13] Han Z, Zhang K, Song W and Liu J 2013 Surrogate-based aerodynamic shape optimization with application to wind turbine airfoils *Aerospace Sciences Meetings* (American Institute of Aeronautics and Astronautics) pp – URL <http://dx.doi.org/10.2514/6.2013-1108>
- [14] Forrester A I J, Sóbester A and Keane A J 2008 *Engineering Design via Surrogate Modelling: A Practical Guide* (John Wiley & Sons, Ltd) ISBN 9780470770801 URL <http://dx.doi.org/10.1002/9780470770801>
- [15] Jonkman J, Butterfield S, Musial W and Scott G 2009 Definition of a 5-MW reference wind turbine for offshore system development Tech. rep.
- [16] Resor B R 2013 Definition of a 5MW / 61.5m wind turbine blade reference model Tech. Rep. SAND2013-2569 Sandia National Laboratories Albuquerque, New Mexico 87185 and Livermore, California 94550,